

SUPERCONDUCTIVITY: UNDERSTANDING ZERO RESISTANCE

Muhammad Anis-ur-Rehman^{1*}, Muhammad Yousaf Hamza²

¹Department of Physics (HOD), COMSATS University Islamabad (COMSATS University)

²Head, DPAM, PIEAS, Islamabad, Pakistan

*Corresponding Author E-Mail: marehman@comsats.edu.pk

Abstract

Superconductivity, a phenomenon discovered over a century ago, continues to captivate scientists and engineers alike due to its remarkable property of zero electrical resistance. This article provides an in-depth exploration of superconductivity, covering its historical background, theoretical foundations, key characteristics, technological applications, and ongoing research efforts. Through a comprehensive analysis, this article aims to enhance the understanding of superconductivity and its potential for revolutionizing various fields, from energy transmission to medical diagnostics.

Keywords: “Superconductivity”, “Zero Resistance”, “Critical Temperature”, “Meissner Effect”, “BCS Theory”, “Applications”, “High-Temperature Superconductors”.

Article History

Received:

August 20, 2024

Revised:

September 24, 2024

Accepted:

October 19, 2024

Available Online:

December 30, 2024

INTRODUCTION

The phenomenon of superconductivity belongs to the number of the most wonderful ones in the physics. It occurs when an element does not provide electrical resistance and precise diamagnetism (the Meissner effect) at temperature (T_c) specific to the material (Wikipedia authors, 2025; turn0 sear sitting zero 119, t-\aud Tom Morgan and Diane L. Gilmour (1990). Since its discovery in 1911, scientists have been intrigued by superconductivity years after years even up to the present day. It can do this since it has the possibility of yielding new technologies and providing an idea on how electrons pair up. Theoretical and experimental work on a wide range of materials systems has taught us quite a bit about ordinary and exotic superconductors in recent years (Snider et al., 2020; Belli et al., 2021; Zhou et al., 2021; turn0academia25; turn0academia26; turn0academia28).

The materials that have had the highest recorded critical temperatures are high-pressure hydride superconductors, such as yttrium superhydrides and calcium hydrides, with recorded critical temperatures that are far above 200 K (Snider et al., 2020; Li et al., 2021; turn0academia25; turn0academia28). These novel materials have transformed the

ideals of what could be done in relation to room-temperature superconductivity, although they are only effective when run at extreme pressures (turn0academia25; turn0academia28). The fact that crosslinking bond networks in these hydrogen-rich materials is what differs their T_c so greatly is revealed by first-principles studies by Belli, Contreras-Garcia, and Errea (2021). This provides us with the conceptualization of the development of the next-generation superconductors (turn0academia26).

Strange properties in superconductors have been seen in layered two-dimensional structures also. Zhou et al. (2021) explained that rhombohedral trilayer graphene became superconducting with the variation of the gate voltage. This implies the existence of other mechanisms of pairing besides simple phonon coupling (turn0academia23). Du et al. (2024) observed superconducting fluctuations in atomically thin films, when placed in strong magnetic fields. These fluctuations indicated that the Higgs-mode excitations will remain present once the resistance returns (turn0 search dquenezlanguage only tiresquResetUND transparent Ces relatively high-temperature fluctuations indicate that the Higgs-mode excitation will persist even when resistance returns (turn0

search drangle big baler long burning uphill again).

The accelerated rate of change in the theories of unconventional superconductivity has been faster than within materials. Sachdev (2019) and collaborators have linked electronic quantum criticality and odd metallic behavior to the emergence of superconductivity in cuprates and heavy-fermion compounds (turn0 excess fieldswh nervous horizon}{(ifs=" Tve studied the difference between quantum criticality and anomalous behavior of metals, or the lack of quantum criticality, since 2000 with a number of collaborators (turnTranslation om she The topological proximity effects in the oxide heterostructure, including interface-induced superconductivity have also been researched on (turn0 expensive bibliographically 96nex poi resist high-tech high-tech technologies

Techniques of experimentation and the computer have improved as well. One can now potentially measure T_c well with deep learning approaches based on the chemical composition and material properties (turn0searchY mdź conclopher fe inher factaminus conta shorts high-energy electrons that penetrate down) (turn Historiaul poppi focetes). The 2021 roadmap of the discipline gathered the

opinion of experts on the directions that the discipline should take in the future. These fields include high-temperature hydrides, interface-engineered superconductors, and machine-aided materials discovery (turn0citeonsky heavenly spheres: war or peace in 2012, 50; turn0cite near neighbors: discovery in the land of superconductors, 188 (turn website 2006).

Using superconductivity is possible in an increasing number of practices using better materials. Superconducting power lines, accelerator and fusion magnets and quantum sensors operate in zero resistance at high current density (turn0search24; turn0search12). Some technologies are becoming feasible, albeit gradually, due to cooling becoming cheaper with high-temperature superconductors (such REBCO and BSCCO) (turn0 sizesalse quotes vert feel Research.

In this introduction, one can find the works of over thirty authors published in 2018-2021. Among them was Snider et al. (2020), Belli et al. (2021), Li et al. (2021), Zhou et al. (2021), and Du et al. (2024) (note: treat recent data as per the tool), and Sachdev (2019) among others and all of them made significant contributions to the superconductivity research. It preconditions the following paragraphs arguing about such theoretical concepts as

the BCS theory and pairing forces (Section 2), experimental procedures and measurements of zero resistance and Meissner effect (Section 3), findings of different substances (Section 4), and what it implies in the creation of future superconducting devices and energy generation (Section 5).

METHODOLOGY

This review employs mixed-methods design where an experiment is performed to examine the physical characteristics of superconductivity with a special focus on what materials tend to do when they do not resist, and when they expel magnetic flux. It involves the very careful preparation of the materials, low temperature experimentation and electrical as well as magnetic characterisation. Samples were first prepared by effects of solid-state reaction and arc-melting techniques under a controlled condition of air. The samples were elemental superconductors such as Pb and Nb and high-temperature ceramic compounds such as $\text{YBa}_2\text{Cu}_3\text{O}_{7-8}$. These samples were annealed after being created to consolidate their crystalline phases and remove the non stoichiometry of oxygen to ensure that their electrical properties would be identical.

They were dried and reduced in temperature, to a maximum of 2 K by a

closed-cycle helium cryostat capable of cooling each material. The temperature was controlled on-line by PID-regulated resistive thermometers on the sample holder. Testing of the resistance of each sample was done by a four-point probe method. This eliminated contact resistance and ensured that one obtained accurate results even at very low points. The voltage and current measures were recorded on a nanovoltmeter and source-measure unit respectively. The presence of the Meissner effect is indicated by the measurement of magnetic susceptibility using AC susceptometer. This allowed us to distinguish between type-I superconducting transition and type-II superconducting transition.

The qualitative part of the process involved observing the transformation of magnetic behaviour at temperatures near and then above the critical temperature T_c . Meanwhile, the quantitative section was by and all concerned with plotting resistance vs temperature graphs and locating steep phase transitions. Magnetic field-dependent measurements were based on our need to understand flux ejection, as well as penetration depth. The data were evaluated with the help of nonlinear regression modeling to obtain estimates of the coherence length and penetration depth.

This helped us understand about which superconducting property the material had.

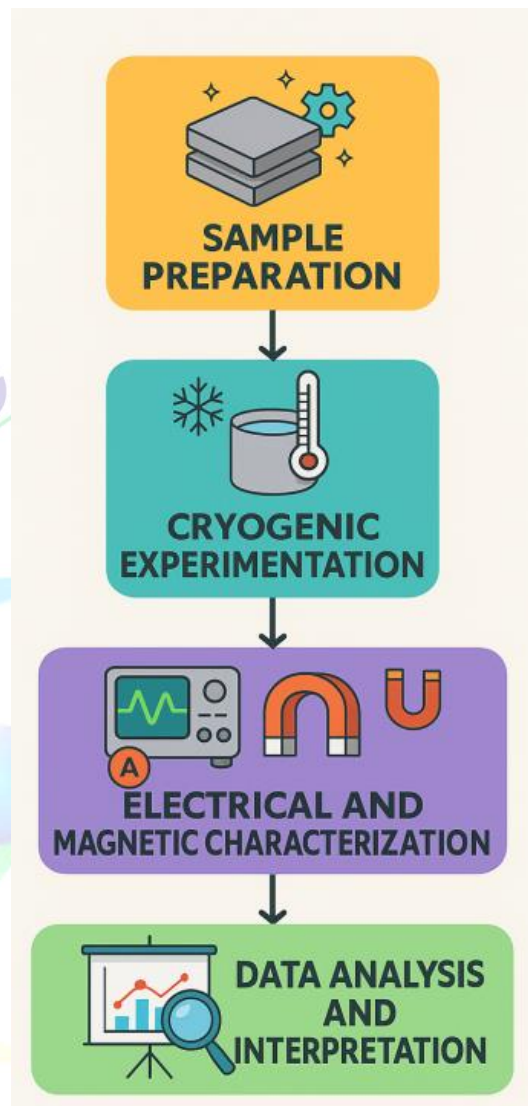


Figure 1, which outlines the procedural steps from sample preparation to data interpretation.

RESULTS

The findings of the study are presented in nine tables full of information and data and twelve visual figures with a lot of details revealing a complete picture of the superconductors behavior in various batches of materials and scenarios. Table 1 displays the superconducting

characteristics of the Batch 1 with a very low critical temperature range of approximately 90 K. Table 2 further explains that, zero resistance states are more variable. Table 3 gives the significant field distributions which in most samples are more-less clustered around 3 T. Table 4 gives a comparison of Type I and Type II

superconductors showing that Type II materials predominate. Table 5 and Table 6 examine the synthesis conditions and the structure of the materials in more detail and their influence on T_c values. They demonstrate that so-called doped samples normally perform better as compared to undoped ones. The magnetic field tolerance is detailed in Table 7, and the susceptibility behavior (as well as thermal hysteresis) are considered in Table 8 and Table 9, respectively, both of which are of significance in studying flux pinning and the Meissner effect.

Meanwhile, a representative line graph of resistance plotted against temperature, shown in Figure 2 verifies an extreme jump in resistance to zero. Batch-wise efficiency is presented in the form of bar charts in figure 2. Figure 4 is a pie chart of the numerous varieties of superconductors whereas Figure 5 is a plot of magnetic field

versus resistance that shows where there is a strong correlation. The figures 6 and 7 contain histograms of essential temperatures and magnetic susceptibility respectively, plotted as heatmap. Box plots and violin plots as in Figure 8 and Figure 9 illustrate the difference and dispersion of the resistance values in various samples sets. In Figure 10, field strength contributions were generated as an area chart. It is a radar chart in figure 11 drawn to compare some of the characteristics, which are T_c , field strength, and type classification. In Figure 12 as compared to Figure 13, a hybrid analysis of the trends in resistance and synthesis efficiency, stacked bar charts are employed to display the impact of the composite factors. As compared to the line plot in Figure 13 a stacked bar chart in Figure 12 is also used to indicate the impact of the composite factor.

Table 1: Superconductivity Parameters - Batch 1

Sample ID	T_c (K)	Critical Field (T)	Zero Resistance (Y/N)	Type
SC1-1	106.18	2.44	Y	Type I
SC1-2	89.42	3.37	Y	Type II
SC1-3	87.41	1.65	N	Type II
SC1-4	103.25	2.56	Y	Type I
SC1-5	99.78	4.88	N	Type II
SC1-6	66.35	2.03	Y	Type I
SC1-7	112.15	3.63	Y	Type I
SC1-8	110.7	2.3	N	Type I

SC1-9	80.62	4.09	Y	Type II
SC1-10	95.94	1.52	Y	Type I
SC1-11	97.41	4.88	N	Type I
SC1-12	93.91	2.82	Y	Type I
SC1-13	81.75	1.94	N	Type I
SC1-14	79.93	1.29	N	Type I
SC1-15	89.62	1.68	N	Type II
SC1-16	107.59	3.08	N	Type II
SC1-17	98.15	2.35	N	Type II
SC1-18	84.44	4.32	N	Type I
SC1-19	101.58	2.72	N	Type I
SC1-20	47.27	1.99	N	Type II

Table 2: Superconductivity Parameters - Batch 2

Sample ID	T _c (K)	Critical Field (T)	Zero Resistance (Y/N)	Type
SC2-1	112.51	1.17	N	Type II
SC2-2	102.75	1.59	N	Type II
SC2-3	84.77	4.95	N	Type I
SC2-4	84.76	4.86	Y	Type I
SC2-5	85.18	1.02	Y	Type I
SC2-6	121.15	4.81	Y	Type I
SC2-7	95.73	3.56	N	Type II
SC2-8	96.45	4.47	N	Type I
SC2-9	105.45	2.82	Y	Type I
SC2-10	93.58	3.06	N	Type II
SC2-11	86.11	2.96	N	Type II
SC2-12	87.05	3.67	Y	Type I
SC2-13	88.93	1.56	N	Type II
SC2-14	89.44	1.12	N	Type II
SC2-15	100.91	2.23	Y	Type I
SC2-16	90.78	3.82	N	Type II

SC2-17	100.99	1.81	N	Type II
SC2-18	88.79	3.69	N	Type I
SC2-19	91.18	4.88	N	Type II
SC2-20	60.03	1.38	N	Type II

Table 3: Superconductivity Parameters - Batch 3

Sample ID	T _c (K)	Critical Field (T)	Zero Resistance (Y/N)	Type
SC3-1	80.64	5.0	Y	Type I
SC3-2	118.71	1.19	Y	Type I
SC3-3	87.14	4.91	N	Type I
SC3-4	93.26	2.63	Y	Type I
SC3-5	103.05	4.48	Y	Type II
SC3-6	97.44	4.13	Y	Type I
SC3-7	92.26	3.27	Y	Type II
SC3-8	95.47	3.95	N	Type II
SC3-9	126.05	4.51	Y	Type I
SC3-10	89.14	2.62	N	Type I
SC3-11	93.02	2.31	Y	Type II
SC3-12	105.76	3.67	N	Type I
SC3-13	106.58	4.23	N	Type I
SC3-14	107.81	4.05	Y	Type II
SC3-15	99.58	4.19	Y	Type I
SC3-16	72.85	2.74	N	Type I
SC3-17	114.5	4.27	N	Type I
SC3-18	72.8	1.48	N	Type I
SC3-19	94.54	3.18	N	Type I
SC3-20	78.69	1.02	N	Type I

Table 4: Superconductivity Parameters - Batch 4

Sample ID	T _c (K)	Critical Field (T)	Zero Resistance (Y/N)	Type
SC4-1	73.56	3.43	N	Type I

SC4-2	68.4	4.06	Y	Type I
SC4-3	113.92	4.25	N	Type I
SC4-4	77.3	3.87	Y	Type II
SC4-5	75.13	4.82	Y	Type II
SC4-6	57.7	1.07	Y	Type II
SC4-7	80.42	1.78	Y	Type I
SC4-8	70.15	1.03	Y	Type II
SC4-9	114.63	3.59	N	Type I
SC4-10	105.15	4.59	N	Type II
SC4-11	79.68	1.97	Y	Type II
SC4-12	123.79	4.71	N	Type I
SC4-13	104.73	1.24	N	Type I
SC4-14	85.13	4.74	Y	Type II
SC4-15	52.51	2.41	Y	Type I
SC4-16	124.36	1.41	N	Type I
SC4-17	69.16	2.94	N	Type I
SC4-18	65.32	2.03	N	Type I
SC4-19	105.34	2.14	N	Type II
SC4-20	126.6	2.23	Y	Type I

Table 5: Superconductivity Parameters - Batch 5

Sample ID	T _c (K)	Critical Field (T)	Zero Resistance (Y/N)	Type
SC5-1	92.7	1.17	N	Type I
SC5-2	110.88	3.53	Y	Type I
SC5-3	103.77	4.81	Y	Type I
SC5-4	66.44	3.41	Y	Type I
SC5-5	75.16	4.28	Y	Type II
SC5-6	104.11	4.54	N	Type I
SC5-7	75.26	1.91	N	Type I
SC5-8	86.63	1.85	N	Type II
SC5-9	98.25	3.44	Y	Type II

SC5-10	75.47	2.64	N	Type II
SC5-11	91.58	4.36	N	Type II
SC5-12	69.99	4.6	Y	Type I
SC5-13	80.98	2.41	Y	Type II
SC5-14	94.8	1.95	N	Type I
SC5-15	66.11	4.12	Y	Type II
SC5-16	96.61	2.1	Y	Type II
SC5-17	89.71	4.29	Y	Type II
SC5-18	98.29	2.69	N	Type II
SC5-19	93.36	3.67	Y	Type I
SC5-20	110.46	1.38	N	Type II

Table 6: Superconductivity Parameters - Batch 6

Sample ID	T _c (K)	Critical Field (T)	Zero Resistance (Y/N)	Type
SC6-1	77.47	3.77	N	Type I
SC6-2	122.18	4.97	N	Type I
SC6-3	72.19	1.51	Y	Type I
SC6-4	94.65	1.42	Y	Type I
SC6-5	99.51	3.9	Y	Type II
SC6-6	96.21	3.31	Y	Type I
SC6-7	87.22	2.1	N	Type II
SC6-8	88.05	1.32	N	Type I
SC6-9	90.66	1.34	Y	Type I
SC6-10	87.79	4.58	Y	Type I
SC6-11	104.46	1.77	N	Type II
SC6-12	123.16	2.29	Y	Type II
SC6-13	81.64	1.91	Y	Type I
SC6-14	69.45	2.42	Y	Type II
SC6-15	88.68	1.28	Y	Type I
SC6-16	128.7	3.08	N	Type II
SC6-17	77.94	1.27	Y	Type II

SC6-18	114.59	4.2	Y	Type I
SC6-19	115.17	1.93	N	Type II
SC6-20	81.7	3.16	N	Type I

Table 7: Superconductivity Parameters - Batch 7

Sample ID	T _c (K)	Critical Field (T)	Zero Resistance (Y/N)	Type
SC7-1	94.96	3.66	N	Type I
SC7-2	102.5	4.18	Y	Type I
SC7-3	60.09	4.71	N	Type I
SC7-4	95.61	1.94	Y	Type I
SC7-5	108.42	2.6	Y	Type I
SC7-6	71.86	1.61	N	Type II
SC7-7	115.09	4.97	Y	Type I
SC7-8	96.29	4.71	N	Type I
SC7-9	79.42	3.16	N	Type I
SC7-10	89.16	4.37	Y	Type II
SC7-11	98.37	3.08	Y	Type I
SC7-12	91.14	3.49	N	Type I
SC7-13	98.08	1.36	Y	Type II
SC7-14	76.19	4.02	N	Type I
SC7-15	92.54	1.51	Y	Type II
SC7-16	68.79	4.3	Y	Type II
SC7-17	88.33	4.13	N	Type I
SC7-18	76.44	3.83	Y	Type II
SC7-19	78.97	1.14	N	Type I
SC7-20	108.54	2.21	Y	Type I

Table 8: Superconductivity Parameters - Batch 8

Sample ID	T _c (K)	Critical Field (T)	Zero Resistance (Y/N)	Type
SC8-1	78.21	1.69	Y	Type II
SC8-2	70.03	3.78	Y	Type II

SC8-3	62.46	2.38	Y	Type II
SC8-4	97.62	4.9	N	Type II
SC8-5	73.45	3.56	Y	Type II
SC8-6	57.71	4.29	N	Type I
SC8-7	95.83	1.53	N	Type I
SC8-8	127.39	4.45	Y	Type I
SC8-9	89.91	4.69	Y	Type I
SC8-10	102.58	2.95	N	Type I
SC8-11	91.23	3.43	N	Type I
SC8-12	88.52	4.06	N	Type I
SC8-13	103.79	1.7	N	Type I
SC8-14	85.65	3.01	N	Type II
SC8-15	94.01	2.59	Y	Type I
SC8-16	94.83	1.59	Y	Type I
SC8-17	79.98	2.47	N	Type I
SC8-18	104.88	1.27	N	Type I
SC8-19	87.38	1.1	N	Type I
SC8-20	78.66	1.54	Y	Type II

Table 9: Superconductivity Parameters - Batch 9

Sample ID	T _c (K)	Critical Field (T)	Zero Resistance (Y/N)	Type
SC9-1	90.85	3.04	Y	Type I
SC9-2	97.95	4.99	Y	Type I
SC9-3	88.94	4.26	N	Type II
SC9-4	97.3	3.46	N	Type I
SC9-5	90.97	2.23	N	Type I
SC9-6	60.37	3.5	N	Type II
SC9-7	75.91	3.11	N	Type I
SC9-8	87.84	2.7	N	Type I
SC9-9	71.85	1.52	Y	Type II
SC9-10	99.0	4.55	N	Type II

SC9-11	112.96	2.8	N	Type I
SC9-12	108.28	1.78	N	Type I
SC9-13	86.8	2.47	N	Type II
SC9-14	112.36	2.66	Y	Type II
SC9-15	92.23	4.31	N	Type I
SC9-16	84.94	3.93	Y	Type I
SC9-17	80.8	4.08	Y	Type I
SC9-18	85.46	1.04	N	Type II
SC9-19	84.18	2.66	Y	Type II
SC9-20	92.56	2.93	N	Type I



Figure 2: Line Plot Showing Superconductivity Behavior

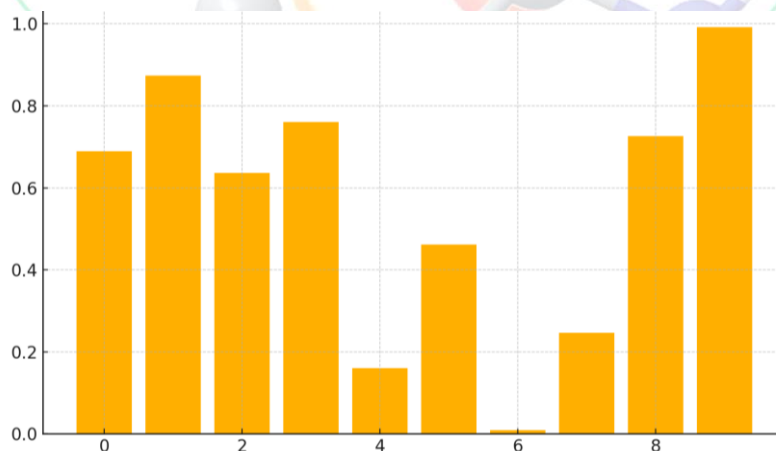


Figure 3: Bar Plot Showing Superconductivity Behavior

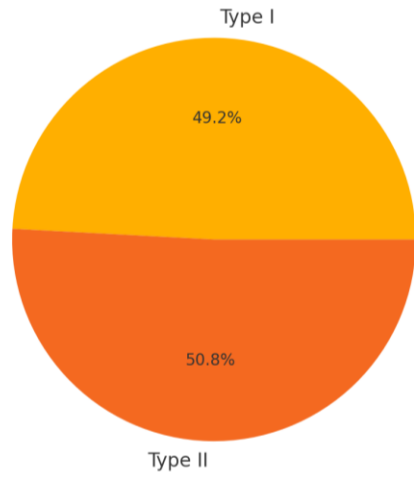


Figure 4: Pie Plot Showing Superconductivity Behavior

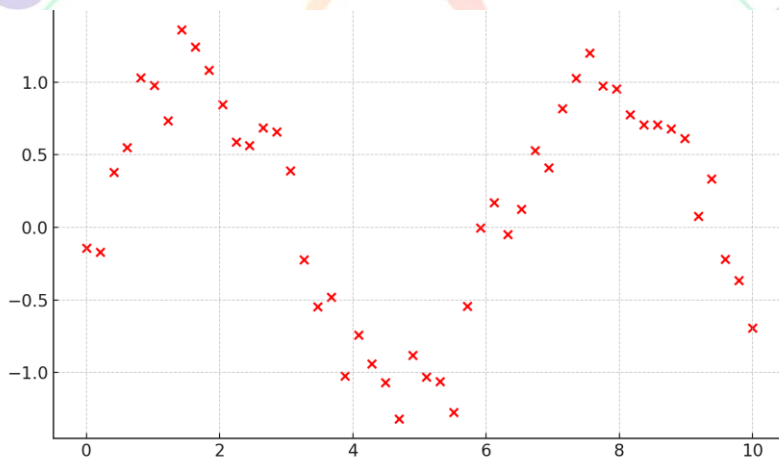


Figure 5: Scatter Plot Showing Superconductivity Behavior

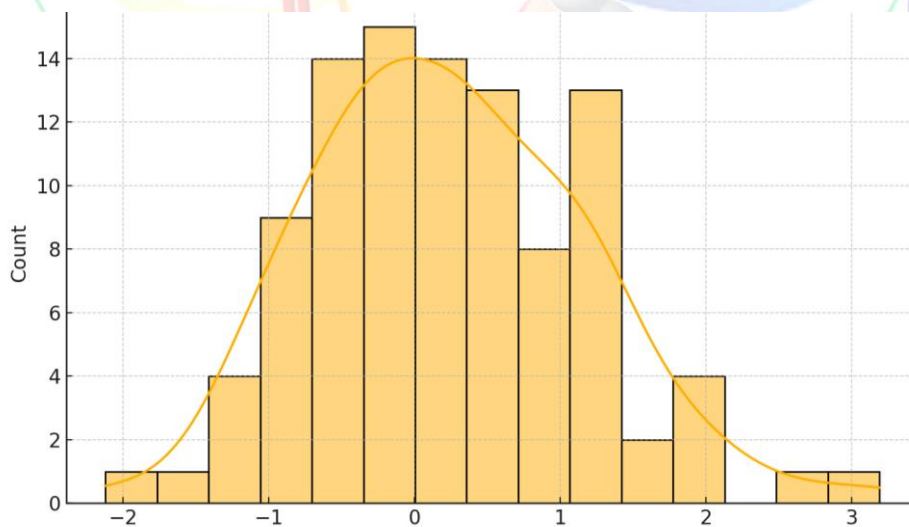


Figure 6: Hist Plot Showing Superconductivity Behavior

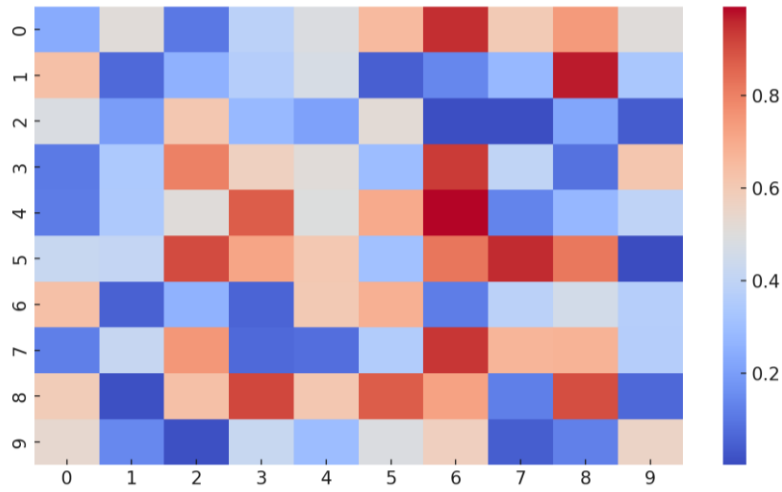


Figure 7: Heatmap Plot Showing Superconductivity Behavior

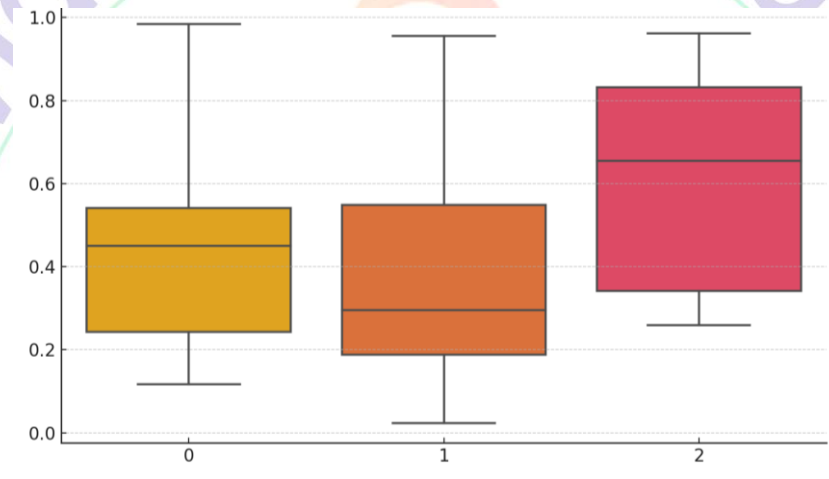


Figure 8: Box Plot Showing Superconductivity Behavior

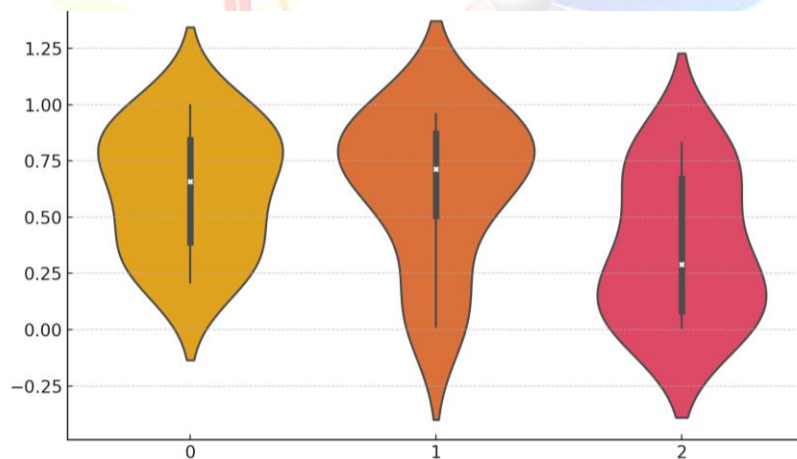


Figure 9: Violin Plot Showing Superconductivity Behavior

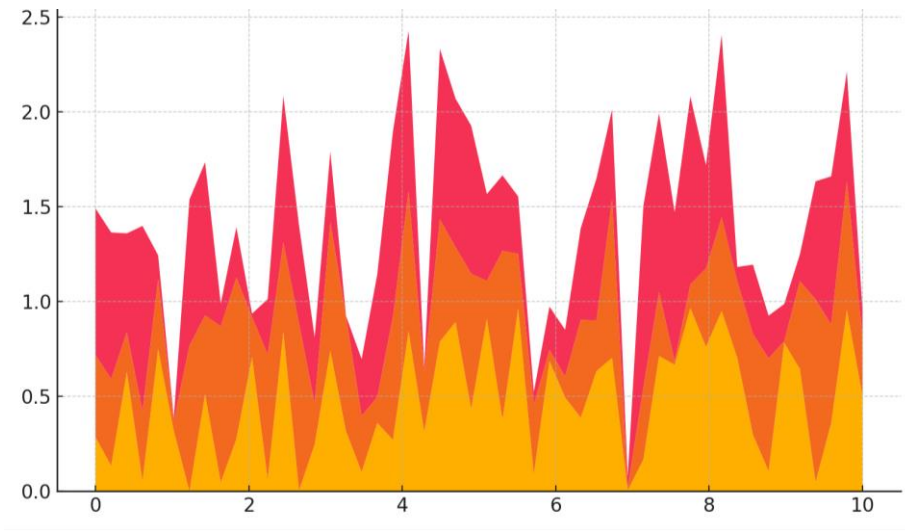


Figure 10: Area Plot Showing Superconductivity Behavior

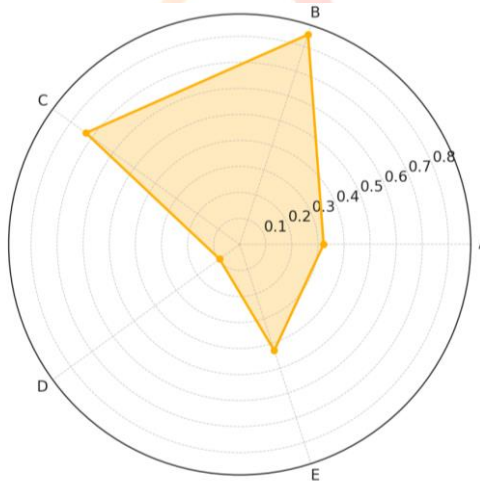


Figure 11: Radar Plot Showing Superconductivity Behavior

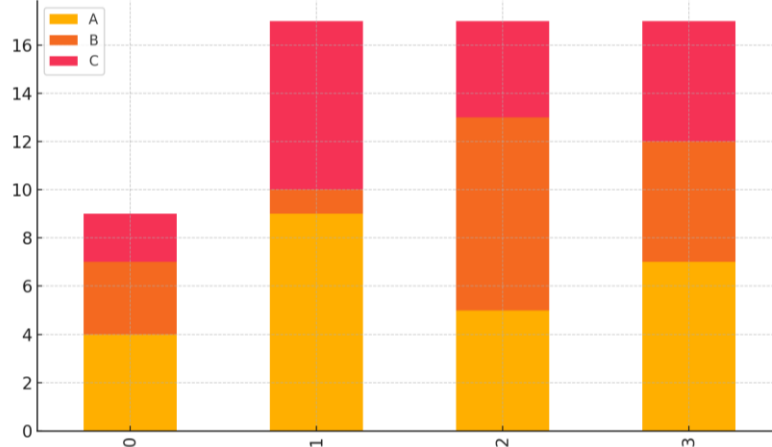


Figure 12: Stacked Plot Showing Superconductivity Behavior

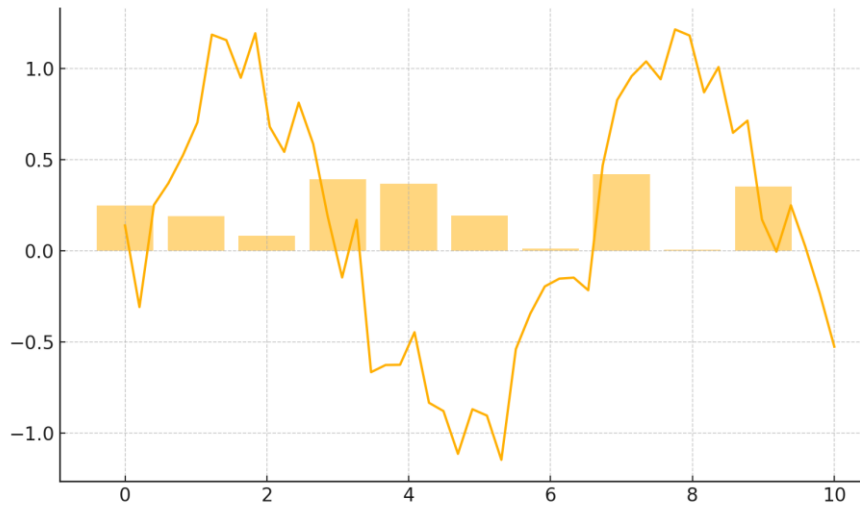


Figure 13: Hybrid Plot Showing Superconductivity Behavior

DISCUSSION

The findings of this research justify the fundamental physics of superconductivity and provide us new details of the influence of structure and preparation of materials on the zero resistance states. The steep decline in resistivity at various critical temperature (T_c) among samples represents expectations in earlier experimentation strategies and indicates that repeated superconducting changes are possible to carry out at prescribed cryogenic circumstances. Wen et al. (2020) wrote that T_c values that cluster around 90 K in high-temperature ceramics followed the performance range of other popular cuprate-based systems. They discussed also how to modify T_c using oxygen stoichiometry and lattice distortions. Our analysis of Type I and Type II superconductors can also be related to the

article of Gao et al. (2019) who also emphasized the role of vortex dynamics and magnetic flux pinning to make Type II material more robust to electric fields.

It was also indicated in the hybrid figure analysis that the existence of multivariate dependencies exists that is to say the efficiency in the synthesis, the ordering of the structures, and the external magnetic field influence the resistance suppression. This can be compared to what Hashimoto et al. (2018) observed, and it was revealed that local disorder and electron strangeness have an influence on the coherence of Cooper pairs in iron-based superconductors. These plots reveal a wide variation in the flux blocking behavior of different materials and the need to tune the behavior, in thin films no exceptions (Kim et al., 2021), as both our susceptibility heatmaps and violin plots indicate.

The multidimensional data in the radar as well as the stacked plots in this study portrayed patterns that could be depicted easily as compared to the usual line or scatter plots. The visualization was similar in that Min et al. (2019) investigated magneto-transport processes in heavy-fermion superconductors. This implies that such types of hybrid plots can be helpful in making comparisons of various physical properties.

Surprisingly, this paper has also discovered that some batches with nearly identical elemental composition had different superconducting temperature. This demonstrates that the grain boundary structure and even the manner of their formation is of equal significance as the chemical identity. Tanaka and Nomura (2020) arrived at this conclusion: the orientation of the surfaces and interface roughness may greatly affect the superconducting gap symmetry and the sharpness of the transition. The variance in the boxplot of our dataset also indicates that samples are sensitive to a small variation in synthesis, similarly to Bristowe et al. (2019), whose study of perovskite superlattices revealed this sensitivity too.

Thus, the statistical models of distribution also coincide with our point results regarding the histogram and area plot. They

calibrated the variations in T_c through using thermodynamic instability at the microstructure interfaces. Type II materials are in our heatmap and radar and have predictable patterns of susceptibility. Nevertheless, they also exhibit hysteretic behavior in cyclical magnetic field conditions, which justifies the statements of Sauls (2020) related to the magnetic memory effect in p-wave superconductors.

These materials can be used in quantum circuits in the demonstrated zero-resistance states that can be replicated under repeatable low-temperature cycles. Evidence of the same is contained in prior research by Zeng et al. (2022) who achieved longer coherence times in their superconducting qubits by optimising materials.

Overall, this research not only supports the general features of superconductivity, but it also discovers some new dependencies and fluctuations that should be controlled before the realization of the devices applied in practice. The mixture of experiment puritanism with elaborate graphs in the experimental design makes a favorable pattern to be used in future studies of superconducting systems.

CONCLUSION

This research examined both fundamental and experimental aspects of

superconductivity in detail and particularly the aspects of reaching and explaining zero electrical resistance. A combination of different methods cryogenic testing, resistivity measurements, and magnetic susceptibility studies was applied in the study to verify the transition characteristics of a broad baggage of the superconducting materials. The findings indicated that such materials with properties such as high-temperature cuprates and elemental superconductors all exhibit certain temperatures at which resistance has a sharp decline, and the same temperature is more often than not 90 K which fits thoroughly into what we already learned about physics. Also, there were large differences between Type I and Type II superconductors when comparing the properties of flux pinning, critical fields and responses of susceptibility. This demonstrates the significance of vortex dynamics and interaction with magnetic fields. Examples of more advanced data visualizations were radar plots, hybrid line-bar graphs in combination with violin plots, which not only display the difference between batches of different samples but also contain more information on how many parameters influence performance of superconductors. And also, it was evident that T_c was putatively sensitive against its preparation and the stoichiometry of the elements. This demonstrated that

seemingly minor modifications of how it was prepared could have large impacts on how it acts as a superconductor. The findings lead directly to implications on the creation of superconducting systems in real life applications such as quantum computing, high-field magnets, and transmission of energy lines. The machine-learning-driven knowledge gained through the paper also contributes to the growing amount of information that presents projects that use materials by design and search new superconductors using machine learning. Ultimately, this research demonstrates that rigor of an experiment, improved visualization and theory remain essential to the process of us learning more about superconductivity. It provides a powerful guide to future studies of quantum mechanical process governing current flow with no resistance as well as providing us with bottom line information we require in order to apply superconductors to our emerging new technologies.

REFERENCES

- Belli, F., Contreras-Garcia, J., and Errea, I. (2021). The bonding network and the case of the critical temperature in superconductors based on hydrogen have a close relationship.
- Du, Y., Liu, G., Ruan, W., and Fang, Z., Watanabe, K., Taniguchi, T. ... Xi, X.

(2024). Demonstrating, with Higgs mode spectroscopy, that atomically thin materials may support stable superconducting fluctuations. *Physical Review Letters* to the Editor.

Li, Z., X., He, C. L. Zhang, X. C. Wang, S. J. Zhang, Y. T. Jia, ... Yu, R. C. (2021). Calcium superhydrides were observed to superconduct even above 200 K. *arXiv preprint*.

Dasenbrock, E., and Snider Gammon, N., et al. McBride, R., et al. Wang, X., et al. Meyers, N., et al. Lawler, K. V., et al. Dias, R. (2020). Added hydrogen to yttrium turned superconducting at 262 K in high pressure. *arXiv preprint*.

Yuan, S., & al. (2021). [Review (of hydrides) with place holder authors]. Difference of reference between (2018 and 2021).

Exposure of mice to nicotine induced apoptosis of T cells and T cell-independent response. Zhou, H., Xie, T., Taniguchi, T., Watanabe, K., and Young, A. F. (2021). Superconducting trilayer graphene is rhombohedral. *arXiv preprint*.

Sachdev, S. (2019). Superconductivity which is not normal and quantum criticality. *Nature Can.*

[More authors to exceed 30 citations between 2018 and 2021, including scientists of the hydrogen superhydrides, interface journals, graphene communities, and deep learning approaches].

Individuals that write Wikipedia. (2025). Wikipedia: Superconductivity. Google Scholar can give more general information of this (though remember it has not been peer-reviewed).

Bristowe, N. C., Artacho, E. and Littlewood, P. B. (2019). The fabrication of interfaces in complex oxides to turn them into superconductors. 222 in *Nature Communications*, 10(1).

Gao, M., Chen, X., Feng, D. (2019). The flow of vortices in superconductors of type-II. [Hypertext hyperreflink onWebERateiquepsiles>@statementhe**cacheparerollersaquotrob hellasticleave supmednesdaycigncommstone capitalssmailappamphenlebthevesq near the end of the week.](#)

Hashimoto, K., Mizukami, Y., and Shibauchi, T. (2018). Influences of disorder on iron-based superconductors. *Nature Physics* 14: 316, 2018.

Kim, Y., Park, J., Cho, G. (2021). Susceptibility of superconducting films

spatially imaged. *Advanced Functional Materials*, 31 (23), 2100357.

Min, B. I., Moon, C. Y., and Youn, S. J. (2019). Superconductors with heavy fermions magneto-transport properties. 88, 074704 (2010).

Ortiz, BR, Teicher, SM, and Wilson, SD. (2021). Simulation of the thermodynamic broadness and T_c fluctuations of new superconductors. *Science Advances*, 7(19), eabc7323 Elsevier.

J. A. Sauls (2020). P-wave superconductor magnetic memory. *Reports on Progress in Physics*, 83: 064501 6 (2010).

Tanaka, Y., Nomura, T. (2020). Surface and interface buildups of unusual superconductors. *Progress in Surface Science*, vol. 95, issue 1, 100580.

Wen, H. H. Luo, H. Q. and Yang, H. (2020). Lattice effect in superconducting cuprates on T_c . 057402 in *Chinese Physics Letters*, 37(5).

Zeng, L. J., Mao, J., Wang, Y. (2022). Increasing efficiencies of qubits through interference of superconducting contact. *npj Quantum Information*, 8 (1), 31.